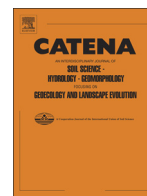




Contents lists available at ScienceDirect

Catena

journal homepage: [www.elsevier.com/locate/catena](http://www.elsevier.com/locate/catena)

## The significance of geomorphological and soil formation research for understanding the unfinished Roman ramp at Masada

Haim Goldfus<sup>a</sup>, Yoav Avni<sup>b</sup>, Roy Albag<sup>c</sup>, Benny Arubas<sup>d</sup>

<sup>a</sup> Ben Gurion University of the Negev, Israel

<sup>b</sup> Geological Survey of Israel, Israel

<sup>c</sup> Architrave Architects, Israel

<sup>d</sup> Hebrew University, Israel

### ARTICLE INFO

#### Article history:

Received 2 September 2015

Received in revised form 17 April 2016

Accepted 18 April 2016

Available online xxxx

#### Keywords:

Masada

Geomorphology

Soil formation

Archeology architectural reconstruction

### ABSTRACT

New multidisciplinary research based on geomorphological investigation and soil survey conducted at the slopes of Masada fort enabled us to reevaluate and question the dramatic events that took place there, in 73/74 CE, according to the 1st century CE Jewish historian, Flavius Josephus. The fort, built on a high elevated and isolated rocky block facing the Dead Sea in Israel, is now on the UNESCO list of World Heritage sites. Here, according to Josephus, a group of Jewish rebels occupying Masada chose to kill each other and die as free people rather than go into captivity. This act took place after the rebels realized that the Roman army, laying a complex assault ramp against the fort of Masada, were breaching its walls. The archaeological finds unearthed at Masada, revealing the daily life of the Jewish rebels and the well-preserved remains of the Roman siege apparatus, seem at face value to complement Josephus' description.

However, our new geomorphological and soil examination of the assault ramp and the natural terrain in its vicinity enable us to clearly separate between the man-made construction and the natural slope environments, and draw a clear boundary between the two. In addition, we conclude that since their formation, they were not subjected to later modification by processes such as natural erosion, slope sliding, or anthropogenic interruptions. As the Roman assault ramp was found to be an uncompleted structure, we conclude that the final scenario of the siege could not have happened as Josephus described it. This meticulous new research confirms our earlier hypothesis that the assault ramp was never completed and therefore could not have been operational. Such a conclusion challenges the common understanding of how the Roman siege of Masada ended.

© 2016 Elsevier B.V. All rights reserved.

### 1. Introduction

This article is dedicated to the memory of Professor Dan Yaalon, a beloved teacher and a colleague, who was a pioneer in the field of desert pedology. Since the early 1950s Dan dedicated his research to the study of arid soils in Israel, the Sinai Peninsula and other arid zones around the world. He was also very interested in the interaction between soils, natural environment and man (see e.g. Yaalon, 2000). The present research comprises a new multidisciplinary research involving soil survey, geomorphological investigation and human activity conducted at the slopes of the famous Masada fort, located at the desert zone of the Dead Sea region, Israel. The results of the soil survey and the study of arid soils in the vicinity of the Roman assault ramp, integrated with data from the fields of archeology, architecture and civil engineering, enable us to re-evaluate and challenge the common understanding of the history of the site, with an emphasis on its end.

#### 1.1. The Masada fort within the Judean desert context

The Masada fort is located at the eastern edge of the Judean desert facing the Dead Sea tectonic depression along the Dead Sea fault zone (Garfunkel, 1981, 2001) (Fig. 1). The Judean desert is a local desert, developed on the down-wind slope of the longitudinal, N–S oriented Judean mountain ridge, ranging in elevation between 800 and 1000 m. This mountain ridge blocks the westerly winds carrying the winter precipitation to the eastern Mediterranean, creating a shortage of precipitation along its eastern slope. This process is the driving force behind the formation of the desert, forming an elongated strip between the Judean Hills in the west and the Dead Sea Lake in the east.

The fort of Masada was built on an isolated horst located on the extreme eastern edge of the Judean desert, circa 500 m above the Dead Sea Lake (Fig. 2A). The fort is surrounded by steep slopes covered by mature colluvial section interfingering with colluvial-alluvial sections that developed on top of abandoned stream terraces. To the east, toward the Dead Sea coastal plain, the lower slopes of Masada block merge with the lacustrine section of the late Pleistocene Lake Lisan (Begin et al., 1974; Fig. 2B). Desert soils, composed of local lithoclasts and fine

E-mail address: [hgoldfus@gmail.com](mailto:hgoldfus@gmail.com) (H. Goldfus).

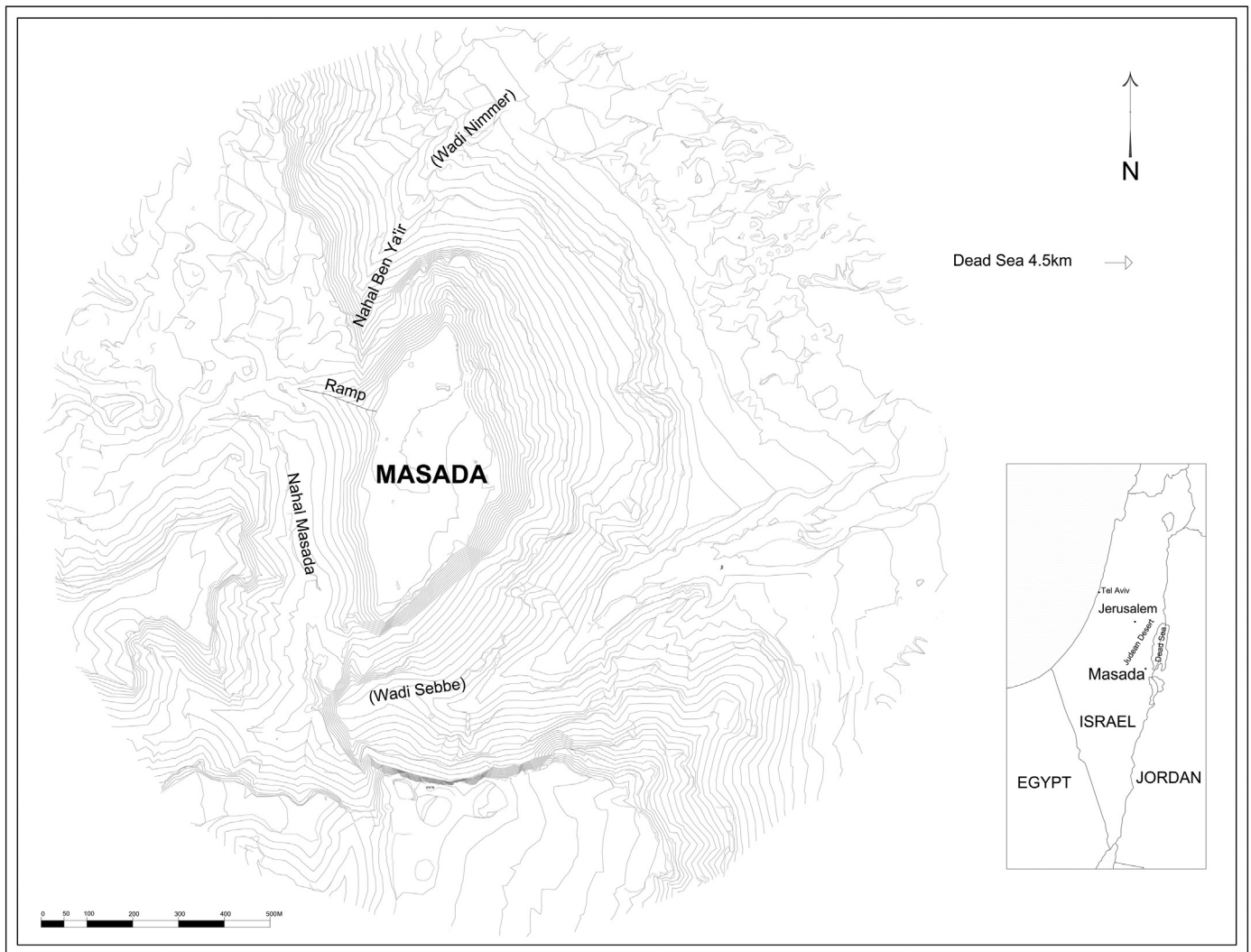


Fig. 1. General location map of the Masada site.

grained aeolian dust (Yaalon and Ganor, 1973; Yaalon, 1981; Dan et al., 1981), were poorly developed on top of the alluvial sediments and the colluvial slopes.

The archaeological site of Masada is on the UNESCO list of World Heritage sites. According to the Jewish historian of the 1st century CE, Flavius Josephus, a group of Jewish rebels, identified by Josephus as Sicarii, besieged the fort of Masada by the Roman army, chose to kill each other and die as free people rather than go into captivity and slavery (JW Bk. 7. 205–406). The archaeological finds unearthed at Masada, revealing the daily life of the Jewish rebels and the well-preserved remains of the Roman siege camps and assault apparatus, seem at face value to complement Josephus' description of the events that took place there (see Ben-Tor, 2009, for an extended summary of the history of Masada and the archaeological finds). According to Josephus's account, Flavius Silva, the Roman commander, ordered the construction of an assault ramp on top of the white natural rock projection jutting out from the cliff of Masada. Since the ramp was neither high nor stable enough, to support siege machines that would enable the breach of the wall of Masada, a massive podium made of perfectly fitted stones was added on top of the ramp. The Romans began their direct attack after an ironclad wooden tower was placed on the latter construction.

The geologist Gill (1993, 2001), following General Lammerer (in Schulten et al., 1933, pp.167–171), questioned part of Josephus' account. He convincingly showed, contrary to what laymen and scholars alike comprehended while reading Josephus' description, that the Roman

ramp was natural to a large extent, and only its upper part was man-made. In addition, Gill concluded that the Romans did not build a massive stone platform atop the ramp. Independently of Gill's study, Goldfus and Arubas (2002), (p. 209) came to similar conclusions following their excavations of the assault ramp in the summer of 1995. However, Arubas and Goldfus (2008, 2010) went further, to assert that the construction of the siege ramp was never completed and therefore it was never operational. Unfortunately, this latter conclusion is either overlooked or worse dismissed (Davies, 2011, Magness, 2012). A lone voice supporting the conclusions of Arubas and Goldfus (2008, 2010) can be found in the recently published book by Mason (2016, pp. 558–75).

In general, the story of Masada has been naively accepted and presented in popular presentations and in the official publications and at Masada. Clearly, Josephus' description of the final acts of the "encounter" between the rebels whereby the Roman ramp was used to breach the walls of Masada, was accepted to a large extent by amateurs and scholars alike (e.g. Roth, 1995; Campbell, 2006, pp. 176–178; Ben-Tor, 2009, p. 292; Gill, 2001, pp. 29–31).

Our present multidisciplinary study aimed to entirely re-examine the validity of Josephus' description by using geomorphological and soil survey methods. We examined the natural slopes and soils developed around the Masada block and in the vicinity of the Roman ramp, and managed to clearly differentiate between the natural, lower part and the man-made upper part. This allowed us to reconstruct with little

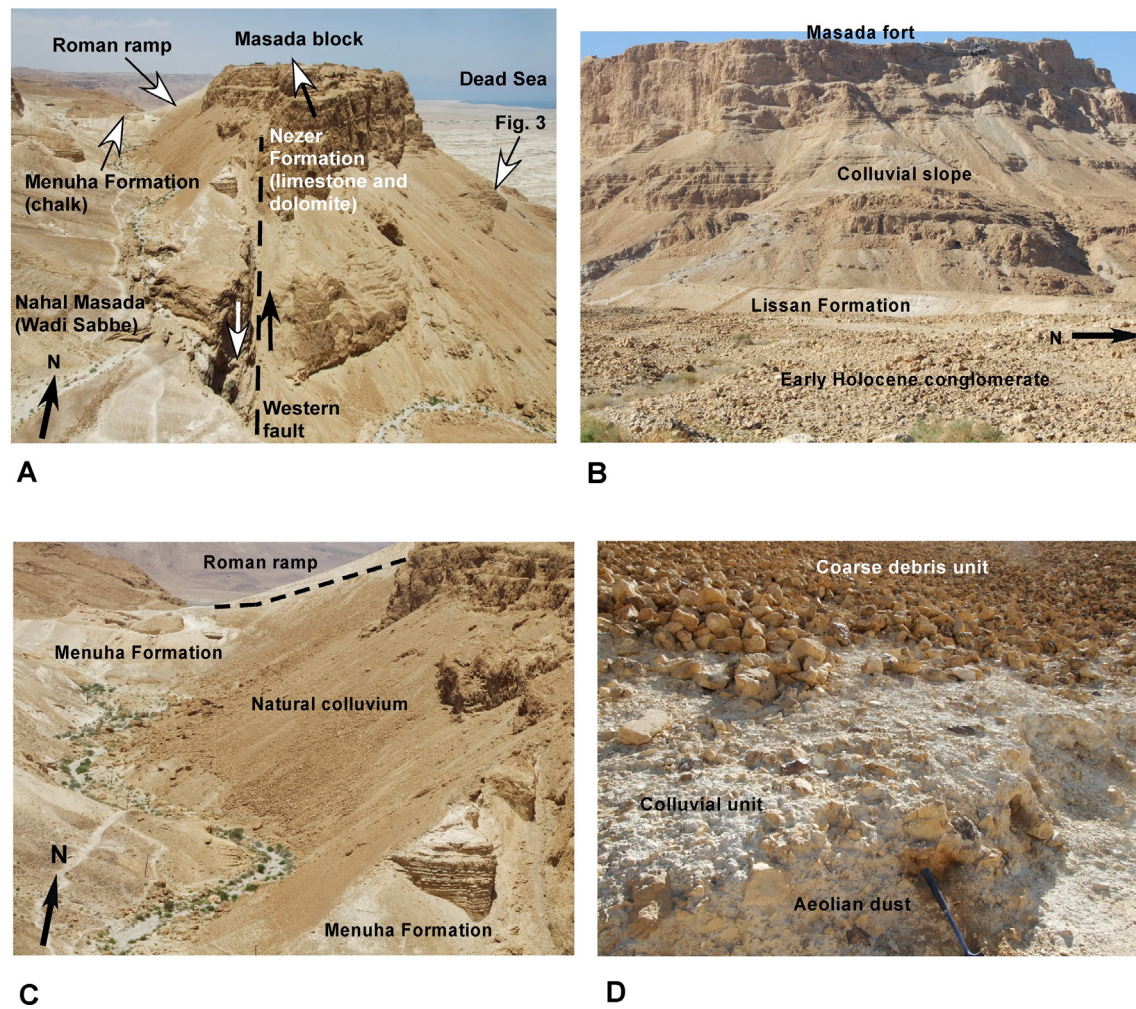


**Fig. 2.** A: A view of the Masada block from the south. Note the Dead Sea in the far background and the western fault separating the Masada block from the Judean Desert (to the left). The location of Fig. 3 is indicated by arrow. B: A view of the eastern slope of the Masada from the east. The lower colluvial section merge with the lacustrine section of the Lisan formation of Late Pleistocene age. The upper lacustrine section is truncated by early Holocene conglomerates deposited at the outlet of Nahal Masada to the Dead Sea coastal plain. C: General view of the western slope of the Masada block from the south. The outcrop of the Santonian Menuha Formation composing the natural spur is seen at the foreground and below the man-made Roman ramp. The boundary between the natural spur and the man-made Roman ramp is indicated by dash line. D: Close look at the western natural slope of Masada in the vicinity of the Roman ramp. The slope is composed of two units: a lower colluvial unit composed of rock fragments integrated with fine lithoclasts and aeolian dust. The upper unit is composed of coarse debris generated from rock falls from the upper cliff of Masada.

doubt the original dimensions and nature of the Roman ramp (natural and artificial) and evaluate any morphological changes that might have occurred there since the 1st century CE.

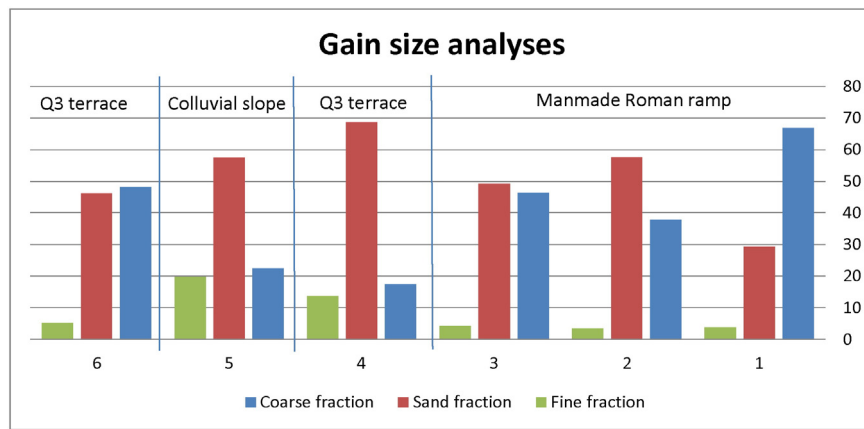
### 1.2. The geology of the site

The Masada fort was constructed on top of a 300 by 600 m massive platform, composed of thick limestone and dolomite layers of Albian to Turonian age (Figs. 2 and 3). The strata comprise the Hevion Formation at its bottom and the Nezer Formation on its top. The block is situated along the main western border fault of the Dead Sea tectonic basin (Fig. 2A; Garfunkel, 1981, 2001; Garfunkel et al., 1981). To its west, the Masada block is separated from the Judean Desert hilly terrain by a N–S fault, causing the uplift of the Masada horst by circa 150 m above its surroundings (Fig. 2A). The top layers of the down-faulted Judean Desert block in the vicinity of Masada consist of the Santonian – Campanian Menuha and the Mishash formations, composed of chalk and flint respectively. As indicated by Gill (1993, 2001), this section constructs a narrow natural spur hill on which the Romans built their assault ramp in 73/74 CE (Gill, 1993, 2001) (Figs. 2A and C).

### 1.3. The geomorphology of Masada

The horst of Masada is a slightly north-south tilted block, which reaches elevation of ca. 60 m a.s.l. at the north and ca. 20 m at its southern extension. The block top stands ca. 500 m above the present level of the Dead Sea. Two small drainage basins drained the western side of the Masada block, diverting on both sides of the natural spur on which the man-made Roman ramp was built: Nahal Ben Ya'ir (previously known as Wadi Nimmer) to the north and Nahal Masada (previously known as Wadi Sebbe) to the south (Figs. 1 and 2A). In the vicinity of Masada the first basin occupies a drainage area of ca. 0.5 km<sup>2</sup>; the second has ca. 5 km<sup>2</sup> and both drain to the Dead Sea via the lower reaches of Nahal Masada. Both drainage basins developed along the major fault line separating the horst of Masada from the nearby hills of the Judean Desert (Fig. 2A).

The slopes of the Masada horst are steep, exposing the massive limestone and dolomite country rock at their near-vertical upper parts, while their lower part is gentler and covered by thick colluvial section (Fig. 2C). This section consists of rock fragments that originated from the upper exposed bedrock, incorporated with aeolian desert dust, brought to the region by winds (Yaalon and Ganor, 1973; Crouvi et al.,



A

Sample no.	Sample name	Total weight	Fine fraction (%)	Sand fraction (%)	Coarse fraction (%)
Ya-1	Roman ramp 1	596.8	3.87	29.27	66.85
Ya-2	Roman ramp 2	342	3.5	57.63	37.71
YA-3	Roman ramp 3	407.8	4.38	49.26	46.34
Ya-4	Terrace Q3	265.7	13.73	68.61	17.53
Ya-5	Colluvial slope	440.9	19.84	57.49	22.49
Ya-6	Terrace Q3	594.1	5.23	46.12	48.14

B

Fig. 3. Grain size distribution presenting the main fractions for samples Ya-1 to Ya-6. A: Graph. Numbers at the bottom line: Sample no. Numbers at the right vertical line: percentage. Fine fraction  $\leq 63 \mu\text{m}$ , Sand fraction  $\leq 2 \text{ mm}$  and Coarse fraction  $\geq 2 \text{ mm}$ . B: Table.

2008, 2015). The eastern slope of the block faces the Dead Sea coastal plain. Along the lower part of this slope the colluvial section merges with the fluvio-lacustrine section of Late Pleistocene (73–14 ka) Lisan Formation (Begin et al., 1974; Fig. 2B), which reach a maximum elevation of 165 m b.s.l. (Bartov et al., 2002). The uppermost layers of the Lisan Formation are slightly truncated by a large fan developed at the outlet of Nahal Masada and Nahal Ben Yair to the Dead Sea coastal plain, reflecting the combined effect of the retreat of the Lisan lake at the end of the Pleistocene and the parallel advance of the fluvial system toward the receding lake (Bartov et al., 2002; Porat et al., 2010; Fig. 2B).

#### 1.4. Present climate

The present climate in the vicinity of Masada is hyper-arid. The mean annual precipitation in the Judean Desert west of Masada is in the range of 100 mm, dropping to <60 mm in the Dead Sea coastal plain. Most of the rain is generated from short-lived winter storms generating rare floods in the drainage basins. The average annual temperatures range between 23 and 25 °C. The maximum daily summer temperatures range between 38 and 40 °C (Israel Atlas, 1970).

#### 1.5. The soils surrounding Masada

Masada's terrain is mostly characterized by exposed rocks, partly covered with shallow soils and very sparse vegetation. The soils in Masada and its vicinity are predominantly Lithic and Typic Torriorthents affected by steep slopes and arid conditions (Regosols), with some Torrifluvents (Fluvisols) developed along the drainage basins (Yaalon and Dan, 1974; Dan et al., 1981; Dan and Yaalon, 1982; Soil Survey Staff, 2014). Another important component, added to the local soils, is

the aeolian dust often labeled as desert loess (Bruins and Yaalon, 1992; Crouvi et al., 2008, 2009, 2010). This component is transported mostly from the Sahara Desert (Yaalon and Dan, 1974; Zilberman, 1992; Crouvi et al., 2008; Faershtein et al., 2016). The dust grains, mainly composed of quartz, are integrated in the alluvial soils developed along the drainage streams in the Negev and the Judean Desert (Dan et al., 1981; Zilberman, 1992; Crouvi et al., 2008, 2009, 2010). This component is clearly seen in the vicinity of Masada (see below).

Considering the prolonged arid environmental conditions in this area (Yaalon, 1981) it is obvious that the present pedogenic setting in the eastern Judean Desert, resembles the one in Roman times. Therefore, evaluation of the soil types and geomorphic structures, such as the colluvial slopes cover developed in the vicinity of the Masada site, can contribute to the characterization of the natural environments versus man-made structures such as the Roman ramp. Clear characterization and separation between the natural slopes, covered by desert soils, and the man-made Roman ramp and its row materials, are critical for evaluation of the original dimensions of the Roman ramp as it was left by the Romans. This step is cardinal for evaluating the archaeological findings and the history of the site.

## 2. Methods

This research uses a multi-disciplinary approach based, on the one hand, on geomorphological and soil investigation and archaeological, and architectural and civil engineering on the other hand. It aims to establish a new understanding of the natural conditions in the vicinity of the Roman assault ramp since it was built and to this day. The geomorphological and soil research was conducted to characterize the natural slopes and soils developed along the western side of Masada block

versus the soils developed on the raw material used by the Romans for their man-made ramp. In order to achieve this goal, the present study applied the following methods:

1. Conducting a geomorphological field survey along the western slope of the Masada block, aiming to evaluate and separate the lithological composition and structure of the natural slopes versus the Roman man-made construction.
2. Conducting a high-resolution soil characterization of the raw materials and soils developed on both, the natural slopes developed on the western side of the Masada block and the man-made Roman ramp. This was based on several methods:
  - A. Basic soil survey, based on samples taken from the soil sections developed on the natural colluvial section system and from the fluvial terrace that merges with the colluvium along Nahal Masada (samples Ya-4–6). In addition, three samples (Ya-1–3) were taken from different sections of the man-made Roman ramp (upper, intermediate and lower) in order to evaluate its composition and its grain size distribution. All samples were first dry sieved to fine ( $\leq 63 \mu\text{m}$ ), sand ( $\leq 2 \text{ mm}$ ) and coarse ( $\geq 2 \text{ mm}$ ) fractions. The results are presented in Fig. 3.
  - B. Particle size distribution (PSD). The samples collected in the previous stage were analyzed and characterized, using laser diffraction in accordance to the procedure used by Crouvi et al. (2008). The Malvern MS-2000 laser diffraction was used for PSD analysis over the particle-size range of 0.02 to 2000  $\mu\text{m}$ . Measurement procedure included dry sieving (below 2 mm) dispersion using sodium Hexametaphosphate solution, stirring for 5 min and ultrasonication for 30 s.  $\text{CaCO}_3$  was not dissolved. Three replicate samples of each sample were then subjected to three consecutive 5-s runs at a pump speed of 1800 RPM. The laser diffraction raw values were transformed into PSD using the Mie scattering model, with optical parameters of  $\text{RI} = 1.52$  and  $A = 0.1$ .
  - C. Thin section analyses: two samples representing the raw material used for the man-made Roman ramp (Ya-2) and the top soil developed on the transition zone between the natural talus and the alluvial terrace Q3 deposited along Nahal Masada (Ya-5) were analyzed and characterized using polarizing microscope.
  - D. SEM and XRD inspection of the diagnostic samples (Ya-2 and Ya-5) representing the raw material used for the man-made Roman ramp and the top soil developed on the transition zone between the natural talus and the alluvial terrace Q3 deposited along Nahal Masada. The investigation was conducted using a Scanning Electron Microscope (SEM), model FEI Quanta 450. The XRD investigation was done using the Philips 1830/3020 X-ray diffractometer.
3. Evaluating the natural erosion features developed on the natural talus system and the man-made Roman ramp since its stabilization. Special attention was given to erosion forms such as gully incision and slope sliding that post-dates the formation and deposition of the natural colluvium and the construction of the Roman ramp and have the potential to deform and alter their original forms.
4. Conducting an inclination survey of the natural slope system along the western margins of the Masada block and of the Roman man-made ramp. The measurements were taken with a Brunton compass. The average accuracy of measurements is in the range of  $1\text{--}2^\circ$ .
5. Conducting longitudinal and cross-sections at the man-made Roman ramp and the natural spur under it, based on a detailed topographic map and with the aid of AutoCAD and Revit programs. It is aimed to evaluate the spatial dimension, the volume of construction, and the steepness of the slopes of the man-made construction atop the natural spur.
6. Comparing and calculating the volume of the artificially-made construction with the volume of missing raw material using CivicCAD program. These two hills, in the close vicinity to the Roman ramp, most likely served as the quarries from which the raw materials of the man-made ramp were taken.

### 3. Results

#### 3.1. The geomorphological survey along the western side of the Masada site

The slopes surrounding the Masada block (Figs. 1, 2A and B) are steep, covered largely by a well-developed natural colluvium that forms an almost continuous veneer. The colluvium is 200–400 m high and 2–3 m thick (Figs. 2B and C). Along the western slope the colluvium rests mainly on the Menuha Formation while on the eastern slope facing the Dead Sea it rests on the Judean Group units (Figs. 2A and B). In few locations, the colluvium is dissected by post-formation erosion, taking the form of minor elongated gullies, 3–5 m deep, that expose the underneath geological section (Fig. 2B). Along the western side of the Masada block and in the vicinity of the Roman ramp, the slopes are covered by thick (circa 3 m) and well-developed colluvium (Fig. 2C). To the south of the ramp the colluvium forms a continuous veneer ca. 570 m long (Fig. 2C), while to the north of the ramp it continues to a distance of circa 300 m before it ends at the steep gorge of Nahal Ben Yair.

#### 3.2. The natural colluvial system

Careful examination of the natural slopes in the vicinity to the Roman ramp indicates that it is totally covered by natural colluvium composed of two sub units:

- 1) Lower unit of colluvial section, 2–3 m thick, composed of local rock boulders and cobbles up to 30–60 cm in diameter, interbedded with fine-grained rock fragments and aeolian dust (Fig. 2D). The combination of the rock fragment and the fine dust forms a well cemented compact unit contributing to its resistance to erosion.
- 2) Upper unit of coarse rock debris and boulders, up to 150 cm in diameter (Fig. 4A), mainly composed of massive dolomite and limestone rock fragments, originating from the disintegration of the upper cliff of the Masada block. This upper unit of local debris accumulated on top of the colluvial section, mainly, after its deposition and stabilization.

#### 3.3. The transition from the colluvial section to the alluvial terraces

The lower part of the colluvium developed to the south of the Roman ramp (Fig. 4B) merges with the fluvial terrace deposited along Nahal Masada (Fig. 4C). The alluvial section is exposed in the terrace is 3–5 m thick; it is composed of a coarse section of poorly sorted boulders and large pebbles derived from the local slopes, composed of a large variety of rocks including chert, limestone, dolomite and chalk. This component is mixed with smaller rock particles and lithoclasts extracted from the local rocky environment mixed with aeolian dust forming lenses (Fig. 4C). The base of the fluvial terraces is not exposed. Yellowish-brown Lithic and Typic Torriorthents (Regosols) have developed on top of the alluvial section and the transition zone to the base of the colluvial section.

#### 3.4. Soils survey, particle size distribution, thin section and SEM inspection on the western natural slope of Masada

Soil survey was conducted along the western slope of Masada in the vicinity of the Roman ramp, about 200 m to its south. On the rocky high grounds of the slopes, the soil is very shallow (1–3 cm) covered by thin biogenic crust. At the lower slopes the Lithic and Typic Torriorthents soil becomes thicker (30–50 cm), and shows a 'loessic groundmass'. The soil is light yellowish-brown silty loam (10 YR 6/4). This type of soil is found also at the top of the abandonment fluvial terraces accumulated along Nahal Masada, and along the transition zone between the fluvial terrace and the lower part of the colluvial section (sample Ya-5 in Fig. 3 and Fig. 4D). At this site a thin layer of desert pavement is developed

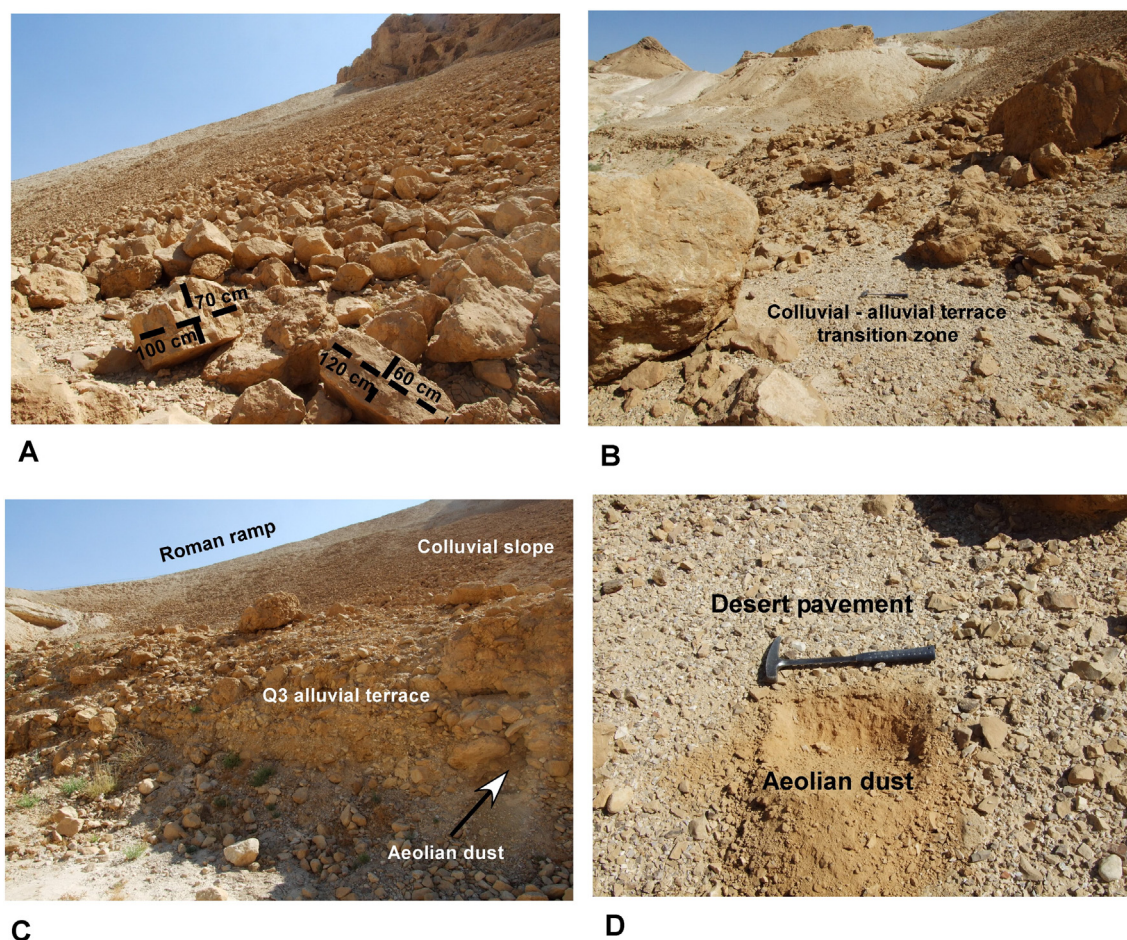


**Fig. 4.** A: Close view of the upper colluvial slope developed along the Masada block slopes unit 200 m south of the Roman ramp. The slope is covered by coarse angular fragments of limestone and dolomite originated from the upper cliff of the Masada block. View from the south; B: The top of the transition zone between the colluvial slope and the alluvial terrace deposited along Nahal Masada. The almost flat surface is covered by poorly developed desert pavement. Scattered boulders are covering the surface resulted from collapse of boulders and rock debris after the fluvial terrace was abandoned; C: Fluvial terrace deposited along Nahal Masada 200 m downstream of the Roman ramp. The terrace is 3–5 m high, composed of poorly sorted boulders and cobbles, poorly cemented by small lithoclast and aeolian dust. This terrace is marked as terrace Q3 and was deposited during the late Pleistocene. An arrow is indicating the location of the Ya-6 sample presented in Fig. 3; D: The top of the alluvial section deposited in the transition zone between the colluvial slope and the Q3 fluvial terrace (see Fig. 4B). The Lithic and Typic Torriorthents soil developed on top of the section is composed of sand and silt particles generated from aeolian dust accumulated below the desert pavement (the location from which sample Ya-5 presented in Fig. 3 was taken).

(Fig. 4D), on top of an almost gravel free silty loess layer of 10–15 cm, enriched in well-sorted aeolian dust grains (Fig. 4D).

The alluvial section in the terraces (Fig. 4C) is composed of rock fragments locally driven from the Nahal Masada basin, composed mainly of limestone and chert pebbles, deposited together with lenses of fine lithoclasts, enriched with aeolian dust that was drifted from the drainage basin during flood events. All these components were integrated together to form the poorly developed Torriorthents soil that developed along the main drainage channels. Two samples (Ya-4 and Ya-6, Fig. 3) represent this deposition environment, taken 1.5 m below its top (Fig. 4C).

These two samples have a wide range of silt and clay concentration ranging between 5.2 and 13.7% (in weight). However, the sample taken from the top of the alluvial section merging with the colluvium (sample Ya-5) has a larger fraction of silt and clays, up to 19.8% (in weight; Fig. 3). All samples from the natural sections have a relatively high percentage (46.1–68.6% in weight) of sandy fraction resulted mainly from disintegration of lithoclasts within the fluvial system. The coarse fraction fluctuates between 48.1 and 17.5%, presenting the poorly sorted fluvial sediment.

The PSD of all naturally developed soils and sediments (samples Ya-4 to 6 in Fig. 5A) has the same general shape of histogram (Fig. 5B) with modes ranging between 30 and 40  $\mu\text{m}$ , typical for the distribution of dust grains in the Judean desert region (Crouvi et al., 2015).

The thin section analysis, the SEM and XRD inspection (Figs. 6 and 7) indicates that most of the silty grains are composed of sub-rounded quartz grains in the size of 30 and 40  $\mu\text{m}$ , originated from aeolian dust. This component is integrated with small particles composed of chert, chalk, limestone and dolomite of various sizes, contributed by the local lithology exposed in the drainage basin of Nahal Masada (Fig. 2A).

### 3.5. The construction of the man-made roman ramp – geomorphological aspects

As indicated by Schulten et al. (1933) and Gill (1993, 2001) the ramp was built by the Romans on top of the natural spur (Figs. 2A and C). It is composed of unsorted rock fragments of chalk, dolomitic chalk with minor components of chert blocks (Fig. 8A) brought to the site from the nearby exposed outcrops of the Menuha Formation. Most of the raw materials were brought to the ramp site in two forms:

1. Solid rectangular blocks, most of them 20–30 cm in diameter, quarried mainly at the base of the natural spur from the intermediate unit of the Menuha Formation. Most of the blocks are composed of limestone, chalky limestone and some chert (Fig. 8A). Among these blocks are some fragments of dolomitic chalk quarried at the dolomitic hill located to the west of the spur and referred to as “the conical hill” (see below).

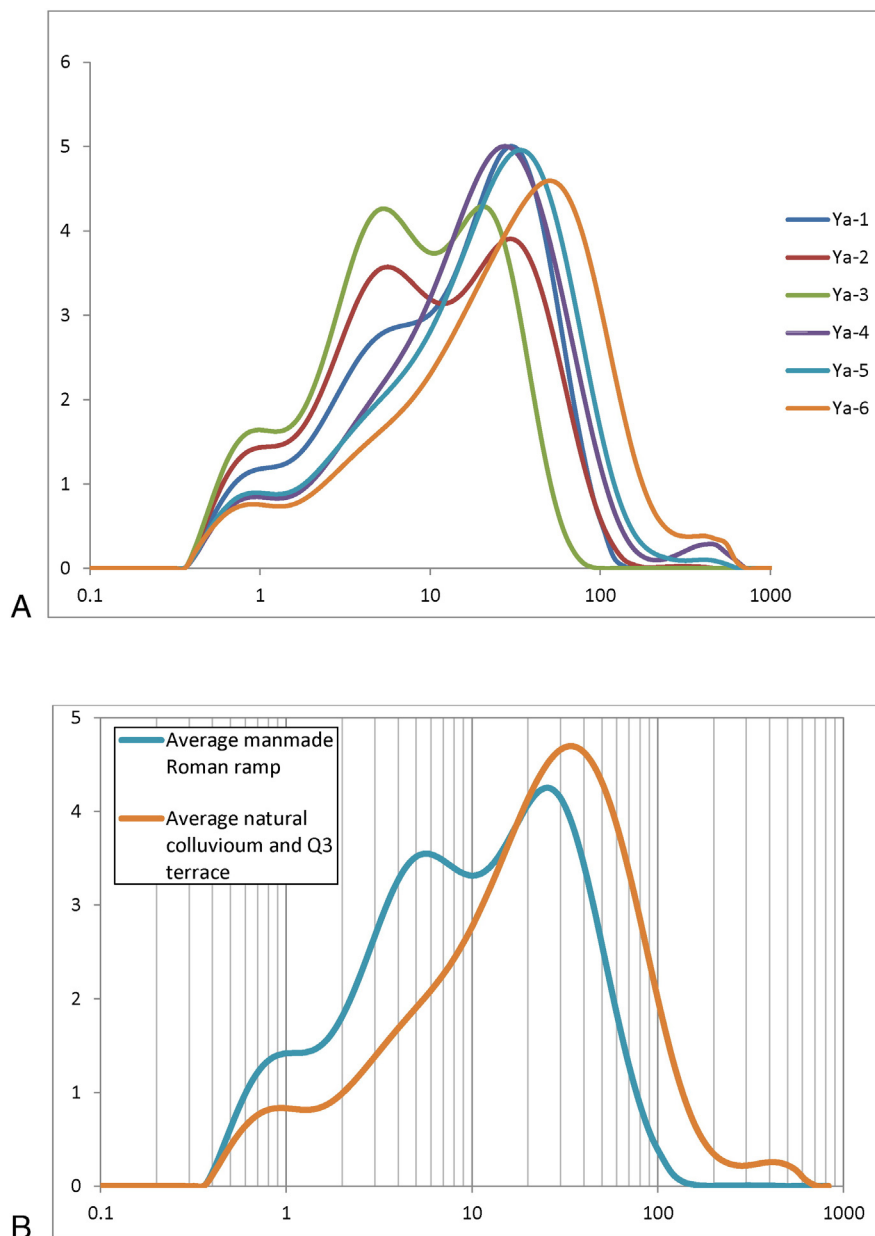


**Fig. 5.** PSD curves presenting the samples taken from the western slopes of the Masada block. A: The total range of PSD. Vertical axis: percentage. Horizontal axis: particle size in microns; B: The separation of the 6 samples presented in Fig. 5A to two main groups: group Ya 1–3 characterizing the raw material used for the man-made Roman ramp and Ya 4–6 characterizing the natural environments of the colluvial slope and the Q3 fluvial terrace.

2. Unconsolidated chalk fragments that served as the matrix holding the rock fragments together (Fig. 8A). Most of this material was quarried from the lower member of the Menuha Formation (see Gill, 1993) that is exposed at the base of the spur. Beside the use of rocks, stones and fragments of chalk, the Romans also used some tree logs and branches (Fig. 8B and C). The use of wood was neither systematic nor extensive. At any rate it seems to have been used more intensively in the lower or bottom parts of the ramp (Fig. 8B). Sparse layers of tamarisk branches and short stumps of palm trees were laid horizontally, one above the other, at irregular intervals (Fig. 8C). At times the logs were inserted diagonally or vertically to the plane of the horizontal layers (Fig. 8C). To the best of our understanding, the use of this technique was meant to secure and stabilize the mass of local chalk and limestone blocks, poured on top of the natural slope along the crust of the spur hill.

3.6. Soil survey, particle size distribution, thin section SEM and XRD inspection of the man-made Roman ramp

The Roman ramp is covered by very thin soil. Its structure is poorly developed and its composition is much closed to the composition of the raw material used for the construction of the man-made ramp having the form of a pedosedimentary groundmass. The soil collected from the upper crust of the ramp is light gray loam (10 YR 8/2). Three samples (Ya-1–3, Fig. 3) were extracted from three different locations along the man-made ramp: lower, intermediate and top. As indicated by the grain size distribution (Fig. 3) these samples contain only negligible fractions of silt and clay (3.5–4.3%, Table 1), while the sandy fraction is in the range of 29.2–57.6% (Fig. 3), and the coarse fraction fluctuates between 37.7 and 66.8%. This distribution reflects the local disintegration of the chalky component to a wide variety of grains and aggregate size, as indicated by the SEM and XRD inspections.

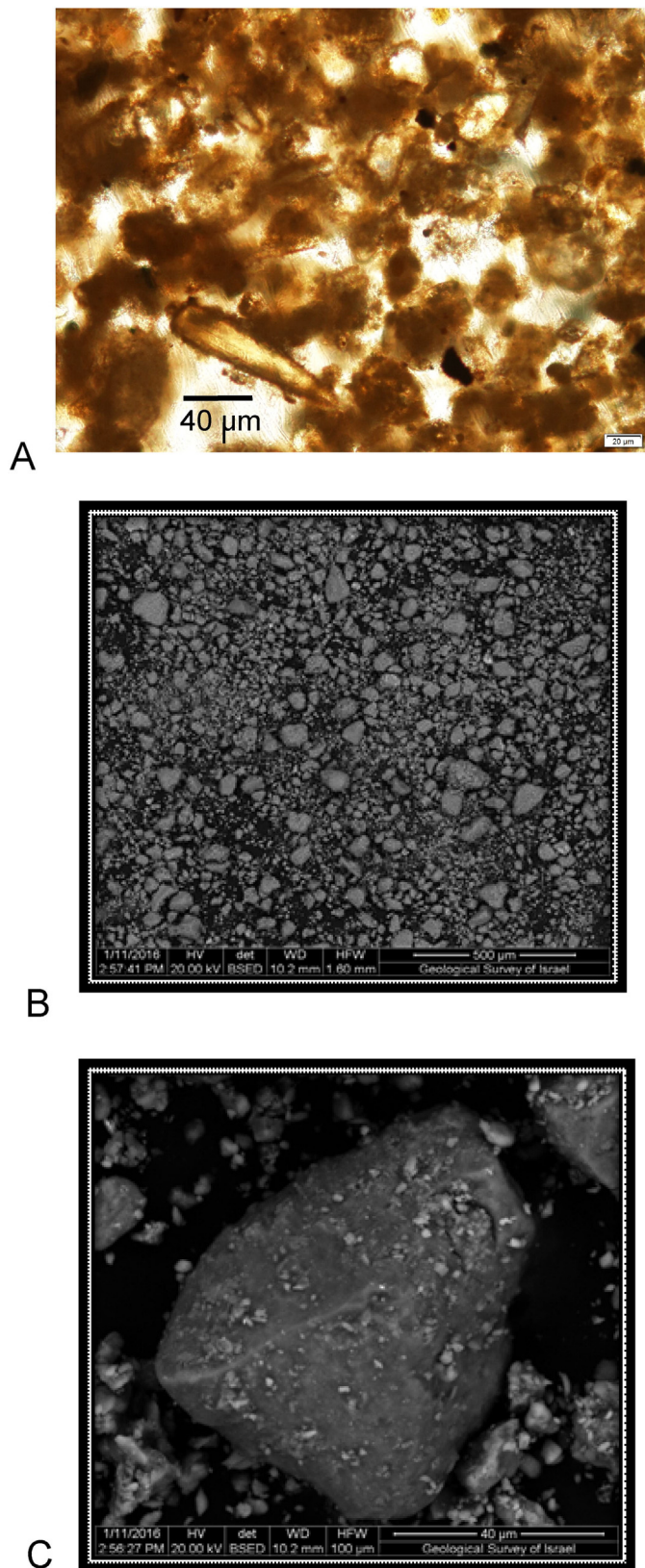


**Fig. 6.** Thin section (A) and SEM inspections (B and C) of the Ya-5 sample characterizing the top of the colluvial section at the western slope of Masada. Note the granular grain assemblage characterizing the aeolian dust. The SEM close inspection is indicating the presence of well-rounded quartz grain (Figure C). (More explanations in text).

The PSD (Fig. 5) indicates that the mean distribution has the shape of a bimodal curve – a fine fraction of 5–7 µm and a coarser one at 20–30 µm. As indicated by inspection with thin section, SEM and XRD, most of the fine-grained particles composing the soils and the ground-mass of the ramp are composed of fine lithoclasts of chalk, made of calcium carbonate as a main component and silica as a minor component, disintegrated from larger chalk fragments containing small individual Foraminifera fossils (Figs. 7 and 9). The contribution of aeolian quartz grains is negligible.

In summary, all these parameters indicates that the poorly developed soils developed on the raw materials use for the man-made Roman ramp differ significantly from the natural colluvial and alluvial soils. In other words, the man-made Roman ramp can easily be distinguished and differentiated from its natural surroundings.

### 3.7. Post-deposition erosion and modification of the Roman ramp construction

In desert environments, including the Negev and the Judean Desert, gully erosion is a well-known feature (Yair and Enzel, 1987; Avni, 2005). This type of erosion is developed along the lower reaches of the two main streams in the vicinity of the Masada site – Nahal Ben Ya'ir to the north, and Nahal Masada to the south of the Roman ramp. Some smaller gullies are developed along the ca. 1200 m long colluvial veneer covering the eastern slope of the Masada block, facing the Dead Sea coastal plain (Fig. 2B). However, along the western slope and in the vicinity of the Roman ramp, almost perfect continued slopes with no gullies are observed (Fig. 2C). In addition, no sign of post-construction erosion or slope sliding is observed on the man-made Roman ramp, a fact mentioned earlier by Gill (1993, 2001). Therefore, clear separation between the natural talus and the man-made Roman ramp is observed with almost no transition zone developed between these two features (Fig. 10).

### 3.8. Geomorphological inclination survey

The inclination survey was carried out in two different slope terrains:

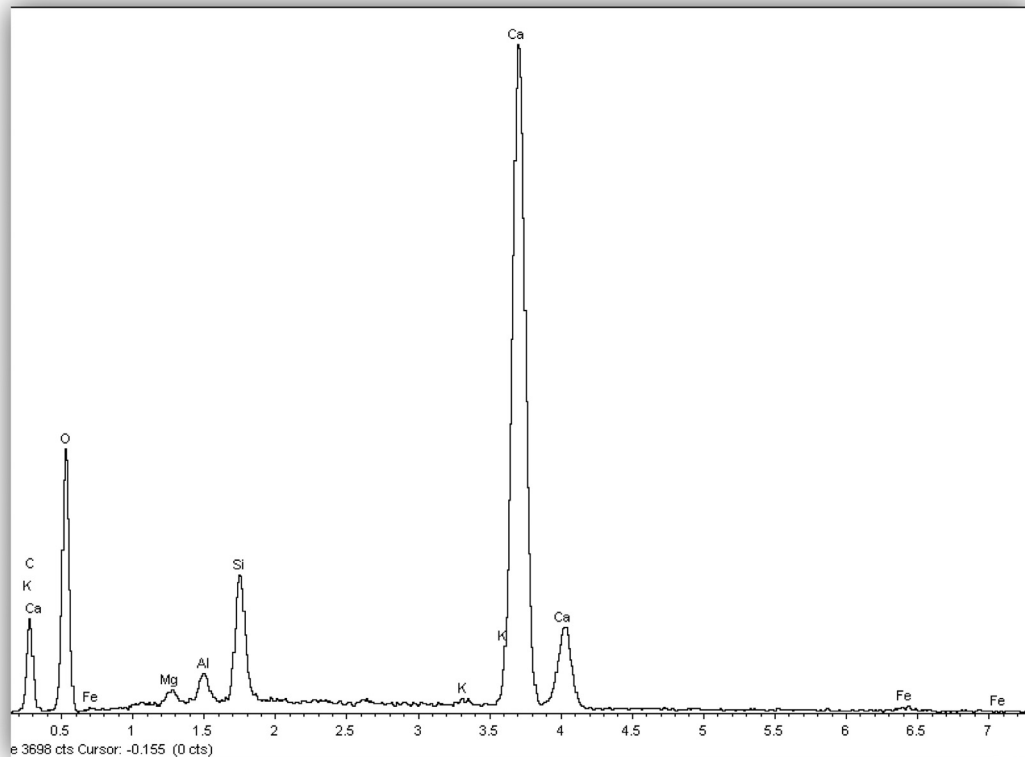
- Perpendicular to the natural colluvial slopes located 200 m on both sides of the Roman ramp.
- Along the two opposite slopes and along the longitude crest of the man-made Roman ramp.

The results of this survey indicate that the two terrains have two distinct inclination ranges. At its middle segment, the natural colluvial slope is inclined 60–63%, with decreasing inclination toward its base, while the side slopes of the man-made Roman ramp are inclined 96–100%. These inclinations are beyond the range of static stability and could be achieved solely by the support of the wooden construction (Fig. 8B and C). The longitude inclination of the man-made Roman ramp along its crest lines is calculated between 31 and 41% (see also below).

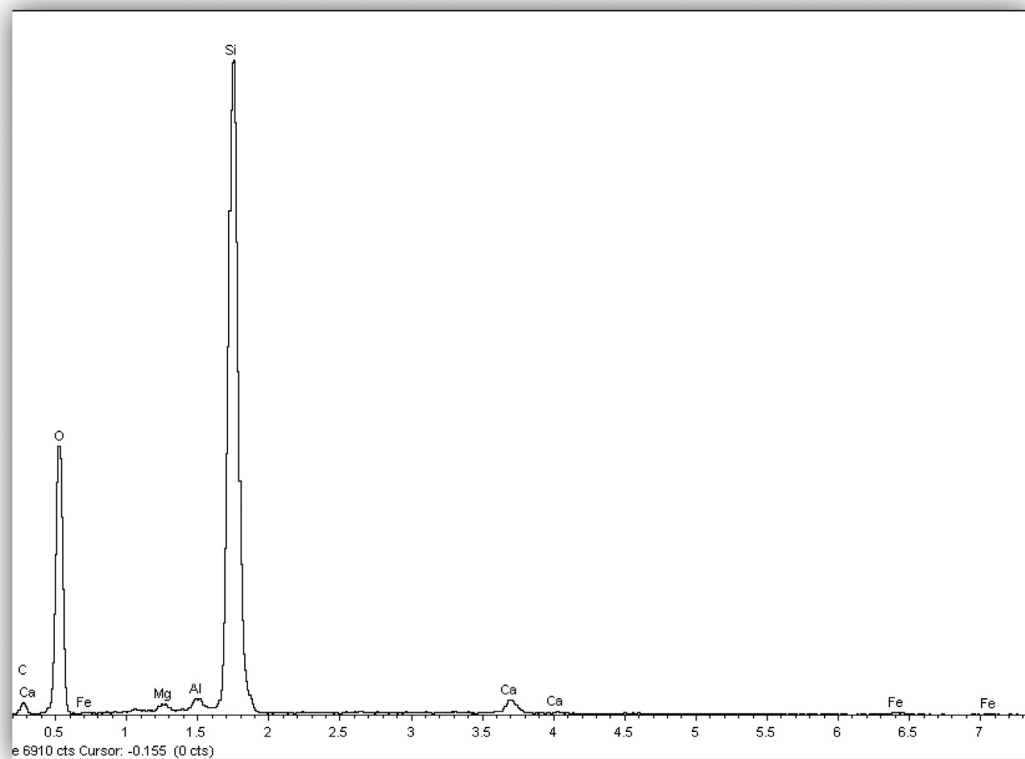
### 3.9. Construction of the roman ramp-architectural and civil engineering aspects

The natural spur and the Roman man-made construction of the assault ramp can be clearly seen in Fig. 11. To comprehend the exact spatial dimension; volume of construction; steepness of the E–W/N–S slopes of the man-made construction (Fig. 12A), and its relation to the relevant features in the natural spur we drew cross-sections along and across these elements and in the immediate vicinity. All these are based on a detailed topographic map (Fig. 12A).



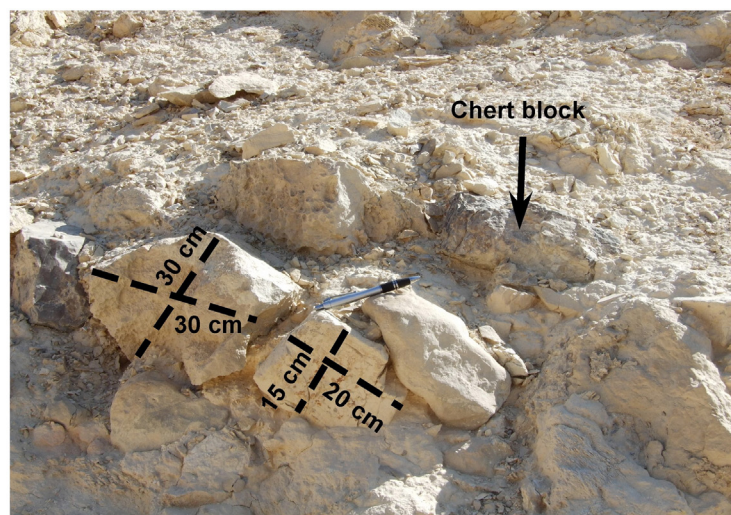


A



B

**Fig. 7.** XRD inspection for the Ya-2 sample (A) characterizing the row material used for the man-made Roman ramp and the Ya-5 sample (B) representing the top of the colluvial section at the western slope of Masada. The high pick observed at the Ya-2 sample is the reflection of the calcite contributed from the chalk of the Menuha Formation while the high pick of silica observed in the Ya-5 sample is the reflection of the aeolian dust abundant in the natural soil environments.



A



B



C

**Fig. 8.** The Roman ramp. A: Close view of the raw material composing the man-made Roman ramp. Note the size of the blocks that were quarried at the base of the ramp from the outcrops of the Menuha Formation. Most of the blocks are composed of chalk. Some chert blocks are also present; B: Sparse short palm tree trunks and tamarisk branches at the southern slope of the man-made Roman ramp; C: tamarisk branches at the northern slope of the ramp.

The longitudinal section (Fig. 12B) was measured and drawn from the Masada cliff (A in Figs. 11 and 12A) along the crest line of the ramp through the 'truncated hill' at the bottom of the ramp (between B—C in Figs. 11 and 12A) referred to as 'white bank' in Gill (2001) and across and beyond the 'conical hill' (C-D). It should be noted that the 'truncated hill' was already noted by General A. Lammerer (in Schulten et al., 1933, pp.167–171). Combining the eight cross-sections (see below, Fig. 12B) and the geomorphological observations (see above) we were able to reconstruct the original 'truncated hill' (presented in pink on Fig. 12B between B and C). In addition we reconstruct the profile and natural ascent to the cliff of Masada (44% gradient) before the arrival of the Romans (Fig. 12B); and the longitudinal slope (31–41% gradient) formed, most likely, as a result of chopping off the 'truncated hill' and part of the 'conical hill' (Fig. 12B).

Drawing and measuring of the eight cross-sections (Fig. 12C/1–8) were based on the geological and geomorphological data presented above and a detailed topographic map. These sections enable us to detect clearly the transitional zone between the natural spur and the man-made ramp. This exact detection is made possible by using reverse engineering of the natural contours that can be detected in the change of the side-slopes and the berms, and by complementing the detailed topographic lines in the plan. Sections 1–5 (Fig. 12C) made along A-B and across the man-made ramp show clearly the artificial fill atop the

natural spur. The sections also show the uneven width of the ramp. While the width at the bottom of the ramp (Fig. 12C/5), i.e. its base, is 46 m, it is only 18 m wide at the base of the upper part of the ramp (Fig. 12C/1). While the height of the fill of the ramp at its bottom (Fig. 12C/5) is 9 m, it is only 5.5 m at the top (Fig. 12C/1). For the operative facet of the ramp, that is, the width of its walking surface, which was allegedly used by soldiers not only for walking but also for pulling or pushing up the battering ram, was 10 m (Fig. 12C/5) at the bottom of the ramp. At its top, closer to the cliffs and the wall of Masada, it was about 1 m wide. One should also recall (see above) that the side slopes (N and S) of the ramp are almost identical and consistent along the whole length (A to B). This fact has direct influence on the operative practicability of the ramp. In other words, the base of the fill directly dictates the operative width of the ramp.

Integrating the longitudinal section (Fig. 12B), the cross-sections (Fig. 12C/6–8 between B and C), the topographic map (Fig. 12A/A), and the geomorphological data (the inclinations of the remaining base of the 'truncated hill') enabled us to reconstruct the shape of the 'truncated hill'. With the aid of AutoCad and Revit we were also able to reconstruct the topography/landscape of the natural ramp prior to the man-made built part of the Roman ramp (Fig. 12A/B, 19 and 20).

By using the model-to-model system in CivilCAD program we also calculated the volume of the raw material quarried from the

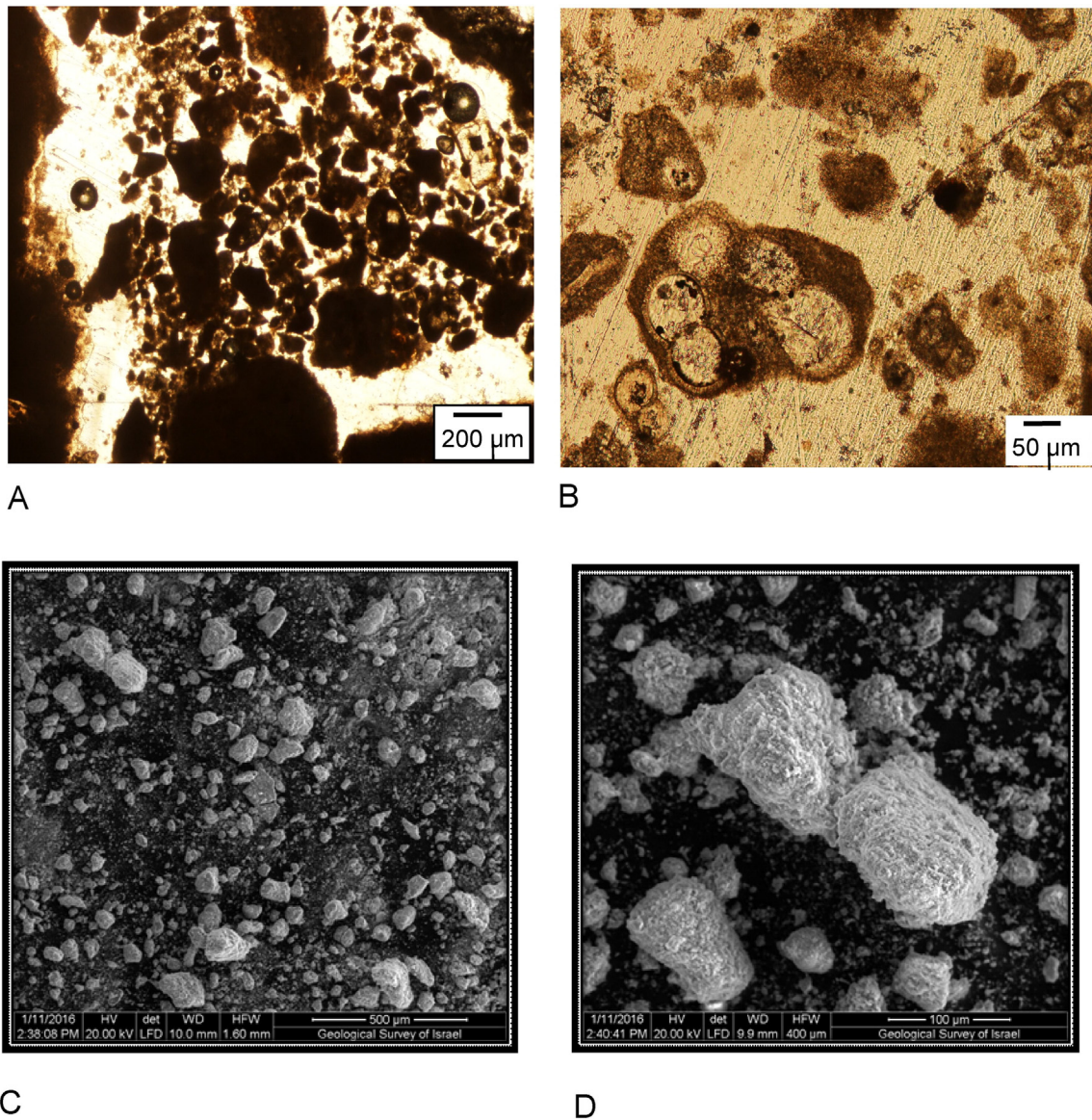


**Fig. 9.** Thin sections (A and B) and SEM inspection (C and D) from sample Ya 2 characterizing the soils developed on the raw material used for the man-made Roman ramp. Note the fragmentation of the chalks into small lithoclasts (A) exposing its Foraminifera fossils assemblage composing the chalk (B). The granular mass of chalk fragments are clearly seen in the SEM (Figures C and D).

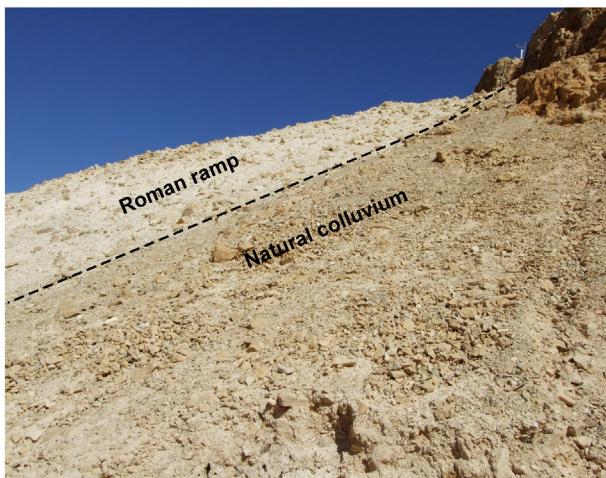


**Fig. 10.** The clear separation between the natural colluvial slope and the man-made Roman assault ramp. View from the south.

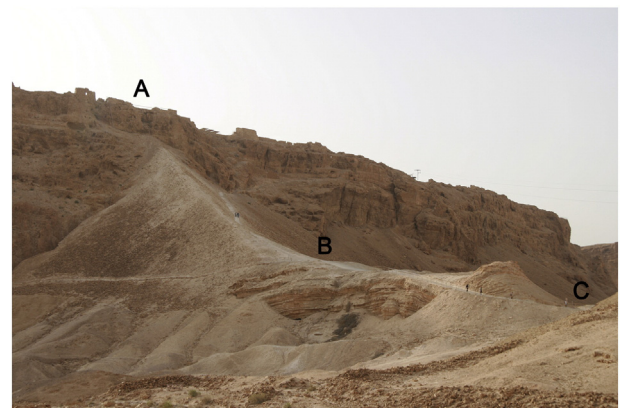
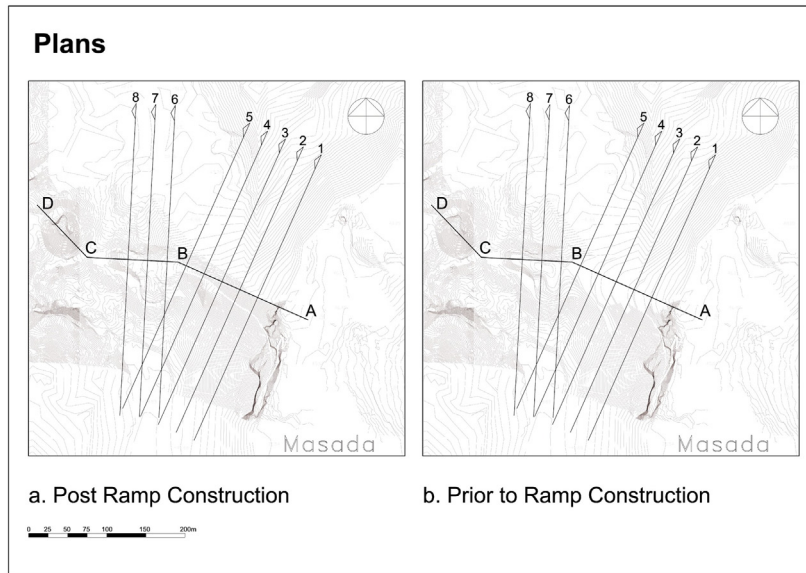
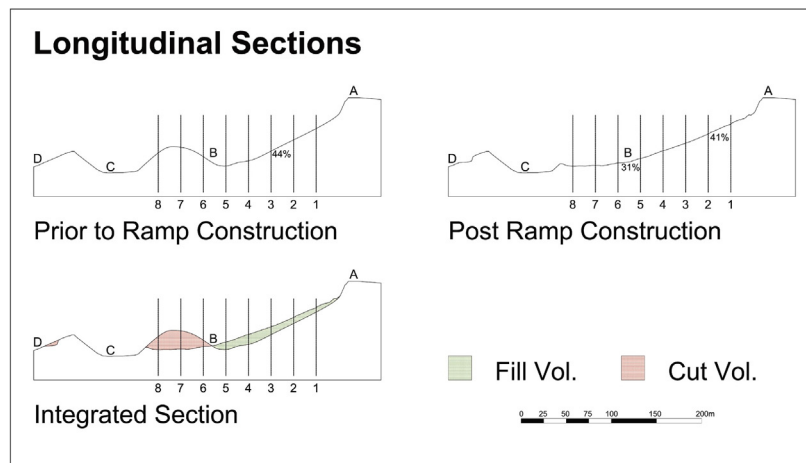


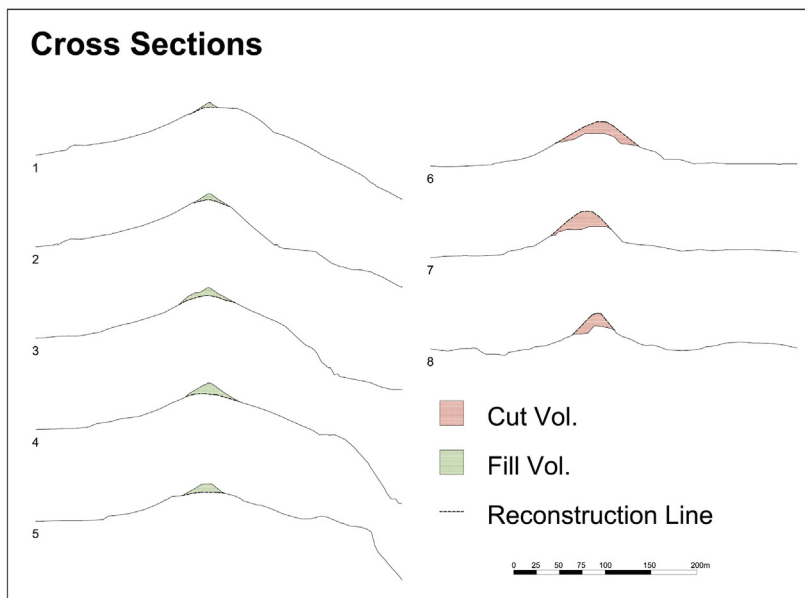
**Fig. 11.** A general view of the natural spur and the Roman ramp as viewed from the northwest. A: the top cliff of Masada; B: the base of the man-made assault ramp and eastern edge of the "truncated hill"; C: the western edge of the "truncated hill".



**A**



**B**



**C**

'truncated hill' (Fig. 12B/B–C) and the 'conical hill' (Fig. 12B/C–D) and the raw materials shifted from these two hills into the artificial ramp (Fig. 12B/A–B).

#### 4. Discussion

The geomorphological and soil survey conducted at the western slope system of the Masada fort, as well as the results of the particle size distribution, thin section analyses, SEM and XRD inspection, and the results of the slope inclination survey presented in this study, enable us to distinguish clearly between the two separate features; the natural slope system and the man-made Roman ramp.

##### 4.1. The soils characteristics

Based on the soil type and the grain size distribution presented in Table 1, a clear separation between the two soil environments can be made. It can be clearly seen that the natural slope environment is enriched with the fine fraction (up to 19.8%) made of aeolian dust material, composed mainly of quartz grains, while in the man-made Roman ramp this fraction has low distribution (3.5–4.3%). The coarse fraction (above the 2 mm) mainly characterizes the soils collected from the Roman ramp, and reflects the disintegration of the chalk raw material, brought to the site from the near-by quarries. The sand fraction, resulted from small lithoclasts of local rock materials, has no diagnostic pattern and fluctuates in all environments.

The results of the PSD, thin sections, SEM and XRD (Figs. 5, 6 and 7) highlights the presence of aeolian dust, enriched in quartz grains, found in the natural colluvial and alluvial sections deposited around the Masada block. Such component was hardly found in the man-made Roman ramp (Figs. 5, 7 and 9). This is a clear indication that the colluvial system surrounding Masada was naturally developed in the course of relatively long geological period, parallel to the deposition of similar colluvial sections and arid soils, developed in the near-by desert environments (Yaalon and Dan, 1974; Dan et al., 1981; Dan and Yaalon, 1982). The quartz grains were originally blown from the Sahara Desert and from the Sinai-Negev sand erg (Crouvi et al., 2008, 2009; Enzel et al., 2008, 2010). Crouvi et al. (2015) described the decrease in particle size, composed of quartz grains at the west-east direction, as particles transported downwind from the Sinai-Negev sand erg. According to their predictions, the quartz grains in the Judean desert, at the vicinity of Masada site, are supposed to be size 30–40  $\mu\text{m}$ . These predictions fit to our observation described here (Fig. 5).

Along the fluvial systems, like at Nahal Masada, the aeolian dust was integrated with locally eroded components such as limestone, dolomite, chalk and chert fragments, derived from local geological outcrops exposed in the drainage basin. This alluvial section was originally deposited within the fluvial channels and was dissected, afterwards, to form the present drainage channels, leaving behind abandonment fluvial terrace, similar to the one which developed along Nahal Masada. Similar processes were widely described in the region of the Negev and the Judean Desert (Yair and Enzel, 1987; Zilberman, 1992; Avni, 2005; Avni et al., 2006, 2012) as well as in other desert environments around the world (e.g. Williams, 2015). Downstream the Nahal Masada, and along the eastern slope of the Masada block, the colluvial and alluvial sections merge with the lacustrine sediments of Lake Lisan (Begin et al., 1974; Bartov et al., 2002; Fig. 2B).

##### 4.2. The formation and age of the natural colluvium and alluvial terraces in the vicinity of the Roman ramp

The synchronous accumulation of the colluvial unit composing the slopes along Nahal Masada, and the alluvial section deposited along Nahal Masada forming a prominent fluvial terrace (marked as Q3 in Figs. 3 and 4C and) enable us to evaluate the timing of the deposition of the combined geomorphologic sequence of slope and fluvial terrace. Both geomorphic elements contain large portions of aeolian dust, composed of a large fraction of quartz grains of 30–40  $\mu\text{m}$ . This composition is typical for the dust accumulated in the desert zone of southern Israel, during the Late Pleistocene (Yaalon and Dan, 1974; Dan et al., 1981; Dan and Yaalon, 1982; Bruins and Yaalon, 1992; Crouvi et al., 2008, 2009, 2015; Enzel et al., 2008, 2010). Similar observations highlighting the importance of the aeolian dust as the primer component of the Late Pleistocene desert soil are described in several studies from different desert regions, including the Judean Desert (Boroda et al., 2011, 2013, 2014), the northern Negev (Crouvi et al., 2008, 2009, 2010; Enzel et al., 2008, 2010) and the Negev Highlands (Avni et al., 2006, 2012; Faershtein et al., 2016).

As the colluvial section along the eastern slopes of the Masada block interbedded with the lacustrine sediments of the Late Pleistocene Lisan Formation (Begin et al., 1974), we conclude that the colluvial unit of the colluvial veneer was formed during the Late Pleistocene, in the approximate time interval of ca. 70–18 ka BP (Bartov et al., 2002). The top of the colluvial section is covered by large boulders and rock falls, accumulated on top of the colluvial unit since it was abandoned, circa 18–14 ka ago. This was followed by the gradual incision of the drainage system down to its present position.

Since the retreat of the lake Lisan at the termination of the Late Pleistocene at circa 14 ka BP, a series of short leaved fluvial terraces were formed as a result of the gradual truncation of the top lake Lisan sequence. This process was active during the latest Pleistocene and the Holocene (Porat et al., 2010; Fig. 2B).

To conclude, the colluvial system developed along the slopes of the Masada block merges with fluvial terrace deposited along Nahal Masada, and with the lacustrine sections of the Lake Lisan. These synchronous geomorphological features suggest that they were formed simultaneously during the late Pleistocene. The fluvial terrace developed along Nahal Masada is identified as the terrace Q3, a terrace that was simultaneously developed along most of the drainage systems in the Judean Desert and the Negev, in accordance with the last glacial event (Zilberman, 1992; Porat et al., 2010; Faershtein et al., 2016). During the Holocene the Masada colluvium and the top sequence of the fluvial terraces along Nahal Masada, as well as the top Lake Lisan sequence, received large amount of boulders (Fig. 4A), which resulted from the rock falls originated from the upper cliffs of Masada block, probably, following heavy rains or earthquakes. These boulders and rock debris gradually accumulated on top of the abandonment terraces and are subjected to gradual disintegration to minor fragment, mainly due to salt weathering process, active in the hyper-arid desert environments (Yaalon, 1981; Dan et al., 1981; Dan and Yaalon, 1982; Amit et al., 2006; Boroda et al., 2011, 2013, 2014).

##### 4.3. The man-made Roman ramp

As mentioned earlier, based on the shallow soil poorly developed on the raw materials and their characteristics, the man-made Roman ramp can be easily distinguished from the natural environments. The Romans

**Fig. 12.** A: Plans - a. post-ramp construction. b. prior-to-ramp construction. A, B and C correlates to what is described in Fig. 11. The line between C and D marks the two sides of the "conical hill"; B: Longitudinal Sections drawn from the Masada cliff along the crest line of the ramp through the "truncated hill" at the bottom of the ramp and across and beyond the "conical hill" (A–D) shows post ramp construction, prior to ramp construction and integrated section; C: Transversal cross-sections and "cut" and "fill" sections of the ramp and "truncated hill". (For interpretation of the references to color in this figure, the reader is referred to the web version of this article.)

made use of two components when building the ramp: the chief component was rocks and stones, locally quarried from the vicinity of the ramp, mainly from the outcrops of the Menuha Formation (Fig. 8A) and trunks and branches of desert trees, mostly growing around Masada (Fig. 8B and C). The chalky fragments disintegrated from the Menuha Formation were found to be a chief component in the thin sections, the SEM and XRD inspections (Figs. 7 and 9). This unique component has its signature in the soil type and the particle size distribution. In addition, the absence of the aeolian dust from the soils developed on the man-made Roman ramp is highly significant. This is the result of the relatively younger age of the Roman ramp and the depletion of the aeolian dust in the late Holocene desert environments (Crouvi et al., 2008, 2009, 2015; Enzel et al., 2008, 2010). These two main observations enable us to clearly distinguish between the natural and man-made environments.

Pouring rocks and stones alone, on the natural spur hill, would not have facilitated a solid mass that would be stable enough to walk on, or carry heavy machinery. However, supporting these rocks and stones, poured on top of the natural slope, along the crust of the spur with wood branches would secure and stabilize the mass of the local chalk and limestone. The use of wood was neither systematic nor extensive but enough to fulfill its purpose. As indicated by the thin section and SEM inspection (Figs. 7 and 9), after the raw material was brought to the site, it was partly disintegrated into smaller particles as weathering process took place during the last two millennia.

#### 4.4. The later modification of the Roman ramp

The two main observations of our research in relation to the present shape of the Roman ramp are:

1. There is clear separation between the natural slopes of the Masada block and the man-made construction. This can be seen in all levels of inspection from the field to the micron scale as indicated in the particle size distribution, thin sections and SEM inspection. These two elements have not mixed ever since the construction of the man-made Roman ramp and there is almost no transition zone between them (Fig. 10).
2. The natural colluvial section along the western slope of the Masada block and the man-made Roman ramp were not modified or eroded by erosion processes after their initial creation. This is clear from the absence of any form of erosion such as gully incision in the vicinity of the Roman ramp. However, gullies, which are a well-known feature in the Judean desert and the Negev, active since the termination of the last glacial period (Yair and Enzel, 1987; Avni, 2005; Faershtein et al., 2016), were observed in other sections of the slopes surrounding the Masada block (see Section 3.2). In addition, no indication of sheet erosion or a significant slide is observed in the vicinity of the ramp. It is also important to emphasize that no evidence of significant tectonic deformation that could have caused the modification of the Roman ramp is observed. This is most evident at the aqueduct bridge, built by king Herold, on both sides of the main western fault of Masada block, long before the construction of the ramp. To the present day, this bridge is intact with no signs of deformation (Fig. 13). As it was built over the most sensitive and seismically hazardous location, we conclude that the ramp, as well as the whole western sector of Masada block, was not affected by any significant seismic deformation since the contraction of the ramp. Therefore, we can conclude that the man-made Roman ramp seen today in the field is virtually to the ramp built by the Romans in the 1st century CE.

#### 4.5. The implications of the cross sections and reconstruction.

The original inclination of the E–W natural spur on which the Romans began their earthworks was 44% (Fig. 12B from B to A). At the bottom of the spur there was a depression located between a hill (Fig. 12A, reconstructed in pink) and the bottom of the spur. In order



**Fig. 13.** A general view of the northern segment of the fault bordering the western side of the Masada block and the aqueduct bridge that was built on both sides of the fault. View from the north. Note the good preservation of the bridge, demonstrating the absence of seismic deformation along the fault or in the vicinity of this site since the construction of the bridge during the 1st century BC. Also note the Roman ramp resting on top of the fault with no sign of deformation. The aqueduct bridge, built by king Herold, stretches on both sides of the main western fault of Masada block, ca. 100 years before the construction of the ramp.

to make the ascent of soldiers and equipment toward the walls of Masada possible, the Romans began to fill the natural depression at the bottom of the spur with rocks quarried from the hill now known as the “truncated hill” and to a lesser extent from the “conical hill” to its west (Fig. 12A). These two hills, in the close vicinity to the Roman ramp, most likely served as the main quarries from which the raw materials of the man-made ramp were taken. The geological and geomorphological examination of the man-made ramp confirms this claim. The quarrying of the “truncated hill” was meant to extend the length of the natural spur, and thus lower the overall incline between B and C (Fig. 12B).

Indeed, by this act the slope between B to A was reduced from inclination of 44% to 41% at the upper part of the ramp and to 31% at its bottom. However, it is clear that the hewing was not completed since the bottom of the “truncated hill” was not finished (Fig. 12B). This did not allow the necessary connection between B and C (see the “post ramp construction” cross section Fig. 12A). The connection between C and A (Fig. 12A/B) would have made the axis somewhat arcuate and longer, but it would have further reduced the slope, between C and A, to 28% average.

Calculating the volumes of the “cut” of the “truncated and conical hills” on the one hand, and the “fill” comprising the man-made ramp on the other hand (with the aid of CivicCAD) shows that the volume of the “cut” was close to 19 km<sup>3</sup> while the “fill” was about 20 km<sup>3</sup>. This allows us to deduce that these two hills were indeed the main source for constructing the Roman ramp. Taking a close look at the topographical map and the cross Sections 1–5 (Figs. 12A and C) allows us to infer that it was possible to expand the operative part of the ramp by extending its base. Section 6–8 (Fig. 12C) clearly shows that it was possible to quarry more filling material in order to reduce the ramp incline and

connect point C to B. In such an instance, the ramp between C to A would have been further extended and could have become operational (Fig. 12B).

## 5. Conclusions

1. The result of our reexamination of the natural spur and the man-made Roman ramp atop it, at Masada, shows beyond any reasonable doubt that both of these features were not affected at all by post-construction erosion, earthquakes, or human intervention. In other words, the structure of the assault ramp, seen today in the field, is almost identical to its original construction by the Romans, 2 k years BP. We claim that since the ramp is very narrow (from 15 m at its bottom, to 1 m wide, at the top of crest); its crust inclination (longitudinal axis) is extremely steep (41% gradient); and it ends 15 m below Masada cliff [at its highest point] with no evidence of any further construction, an operational ramp was never materialized. In other words, the Roman ramp at Masada was never operational and could not have been functional for the reasons for which it was built.
2. Any archaeological data that have been related to military interaction between the zealots and the Roman army, must leave the unfinished Roman-ramp opera out of the play.

## Abbreviations

JW = The Jewish War by Flavius Josephus. English translation by H. St. J. Thackeray. Vol. 3 Books IV–VII (Loeb Classical Library 210), Cambridge, Mass. and London, 1990 reprint

## Acknowledgments

The authors would like to thank: Prof. Dan Bauman for affirming our preliminary observations long before the present study; to Anna Albag, for making available mapping and survey data and elaborations; We also wish to thank Yacov Refael from the Geological Survey of Israel for his assistance and Danny Itkin for his comments and suggestions on the soil issues for the revised manuscript. Special thanks go to Steve Mason and Tamar Fox who improved the text in no time.

## References

- Amit, R., Enzel, Y., Sharon, D., 2006. Permanent quaternary aridity in the southern Negev, Israel. *Geology* 34, 509–512.
- Arubas, B., Goldfus, H., 2008. Masada - the Siege System. The New Encyclopedia for Archaeological Excavations in the Holy-Land. Israel Exploration Society, Jerusalem, pp. 1937–1939.
- Arubas, B. and Goldfus, H., 2010. Masada -the Roman Point of View in Light of New Excavations at the Siege Works, Or-Le-Mayer, Studies in Bible, Semitic Languages, Rabbinic Literature and Ancient Civilizations Presented to Mayer Gruber on the Occasion of Sixty-five Birthday, Shamir, Yona (Ed.), (Beer-Sheva. pp. 19–32 (Hebrew), p. 223 (Eng. abstract).
- Avni, Y., 2005. Gully Incision as a Key Factor in Desertification in an Arid Environment, the Negev Highlands, Israel. 63. *Catena*, pp. 185–220.
- Avni, Y., Porat, N., Plakht, J., Avni, G., 2006. Geomorphologic changes leading to natural desertification processes versus anthropogenic land conservation in an arid environment, the Negev Highlands. *Isr. Geomorphol.* 82, 177–200.
- Avni, Y., Porat, N., Avni, G., 2012. Pre-farming environment and OSL chronology in the Negev highlands, Israel. *J. Arid Environ.* 86, 12–27.
- Bartov, Y., Stein, M., Enzel, Y., Agnon, A., Reches, Z., 2002. Lake levels and sequence stratigraphy of Lake Lisan, the late Pleistocene precursor of the Dead Sea. *Quat. Res.* 57 (1), 9–21.
- Begin, Z.B., Ehrlich, A., Nathan, Y., 1974. Lake Lisan, the Pleistocene precursor of the Dead Sea. *Isr. Geol. Surv. Bull.* 63 (30 pp.).
- Ben-Tor, A., 2009. Back to Masada. Israel Exploration Society, Jerusalem.
- Boroda, R., Amit, R., Matmon, A., Team, A.S.T.E.R., Finkel, R., Porat, N., Enzel, Y., Eyal, Y., 2011. Quaternary-scale evolution of sequences of talus flatirons in the hyperarid Negev. *Geomorphology* 127, 41–52.
- Boroda, R., Matmon, A., Amit, R., Haviv, I., Porat, N., Team, A.S.T.E.R., Rood, D., Eyal, Y., Enzel, Y., 2013. Long-term talus flatirons formation in the hyperarid northeastern Negev, Israel. *Quat. Res.* 79, 256–267.

- Boroda, R., Matmon, A., Amit, R., Haviv, I., Arnold, M., Aumaitre, G., Bourles, D.L., Kaddadouch, K., Eyal, Y., Enzel, Y., 2014. Evolution and degradation of flat-top mesas in the hyper-arid Negev, Israel revealed from <sup>10</sup>Be cosmogenic nuclides. *Earth Surf. Process. Landf.* <http://dx.doi.org/10.1002/ESP.3551>.
- Bruins, H.J., Yaalon, D.H., 1992. Parallel advance of slopes in Aeolian loess deposits of the northern Negev, Israel. *Isr. J. Earth Sci.* 41, 189–199.
- Campbell, D., 2006. *Beseiged: Siege Warfare in the Ancient World*. Osprey Publishing, Oxford and New York.
- Crouvi, O., Amit, R., Enzel, Y., Porat, N., Sandler, A., 2008. Sand dunes as a major proximal dust source for late Pleistocene loess in the Negev Desert, Israel. *Quat. Res.* 70, 275–282.
- Crouvi, O., Amit, R., Porat, N., Gillespie, A.R., McDonald, E.V., Enzel, E., 2009. Significance of primary hill top loess in reconstructing dust chronology, accretion rates, and sources: an example from the Negev Desert Israel. *Journal Geophysical Research-Earth Surface* 114, 1–16, F02017.
- Crouvi, O., Amit, R., Enzel, Y., Gillespie, A.R., 2010. Active sand seas and the formation of desert loess. *Quat. Sci. Rev.* 29, 2087–2098.
- Crouvi, O., Enzel, Y., Ben-Dor, Y., Amit, R., 2015. Field Trip Guidebook, the Batsheva de Rothschild Seminar on Atmospheric Dust, Dust Deposits (Loess) and Soils in Deserts and Desert Fringe. *GSI/22/2015*.
- Aridic Soils of Israel: Properties, Genesis and Management (with Preface by Dan H. Yaalon). In: Dan, J., Gerson, R., Koyumdjisky, H., Yaalon, Dan H. (Eds.), Special Publication 190, Bet Dagan, Israel. Agricultural Research Organization, Institute of Soils and Water.
- Dan, J., Yaalon, D.H., 1982. Automorphic Saline Soils in Israel. In: Yaalon, Dan H. (Ed.), *Aridic Soils and Geomorphic Processes: Proceedings of the International Conference of the International Society of Soil Science, Catena Supplement 1*. Catena Verlag, Braunschweig, pp. 103–115.
- Davies, G., 2011. Under siege: the roman Field works at Masada. *Bull. Am. Sch. Orient. Res.* 362, 65–83.
- Enzel, Y., Amit, R., Dayan, U., Crouvi, O., Kahana, R., Ziv, B., Sharon, D., 2008. The climatic and physiographic controls of the Eastern Mediterranean over the late Pleistocene climates in the southern Levant and its neighboring deserts. *Glob. Planet. Chang.* 60, 165–192.
- Enzel, Y., Amit, R., Crouvi, O., Porat, N., 2010. Abrasion-derived sediments under intensified winds at the latest Pleistocene leading edge of the advancing Sinai-Negev erg. *Quat. Res.* 74, 121–131.
- Faershtein, G., Porat, N., Avni, Y., Matmon, A., 2016. Aggradation–incision transition in arid environments at the end of the Pleistocene: an example from the Negev highlands, Southern Israel. *Geomorphology* 253, 289–304.
- Garfunkel, Z., 1981. Internal structure of the Dead Sea leaky transform (rift) in relation to plate kinematics: Tectonophysics, v. 80, pp. 81–108.
- Garfunkel, Z., 2001. The nature and history of motion along the Dead Sea Transform (Rift). In: Horowitz, A. (Ed.), *The Jordan Rift Valley*. A.A. Balkema, Lisse, the Netherlands, pp. 627–651.
- Gill, D., 1993. A natural spur at Masada. *Nature* 364, 569–570.
- Garfunkel, Z., Zak, I., Freund, R., 1981. Active faulting in the Dead Sea rift. *Tectonophysics* 80, 1–26.
- Gill, D., 2001. It's a natural: Masada ramp was not a roman engineering miracle. *Biblic. Archaeol. Rev.* 22–31, 56–57 (Sep/Oct).
- Goldfus, H., Arubas, B., 2002. Excavations at the Roman Siege Complex at Masada–1995. In: Freeman, P., Bennett, J., Fiema, Z., Hoffmann, B. (Eds.), *Limes XVIII: Proceedings of the XVIIIth International Congress of Roman Frontier Studies, Held in Amman, Jordan (September 2000)* 2. BAR International Series 1084, Oxford, pp. 207–214.
- Israel Atlas, 1970.
- Magness, J., 2012. A Reconsideration of Josephus' Testimony about Masada. In: Leiden, M. Popović, Boston (Eds.), *The Jewish Revolt against Rome: Interdisciplinary Perspectives*, pp. 343–359.
- Mason, S., 2016. *A History of the Jewish War, A.D.* Cambridge University Press, New York, pp. 66–74.
- Porat, N., Amit, R., Enzel, Y., Zilberman, E., Avni, Y., Ginat, H., Gluck, D., 2010. Abandonment ages of alluvial landforms in the hyperarid Negev determined by luminescence dating. *J. Arid Environ.* 74, 861–869.
- Schulten, A., Lammerer, A., Paulsen, R., Regling, K., Schramm, E., 1933. Masada Die Burg Des Herodes Und Die römischen Lager Mit Einem Anhang: Beth-Ter. *Zeitschrift Des Deutschen Palästina-Vereins* 56 Heft 1/3, pp. 1–185.
- Staff, Soil Survey, 2014. *Keys to Soil Taxonomy*. 12th ed (United States Department of Agriculture Natural Resources Conservation Service).
- Roth, J., 1995. The length of the siege of Masada. *Scr. Class. Isr.* 14, 87–110.
- Williams, M., 2015. Interactions between fluvial and eolian geomorphic systems and processes: example from the Sahara and Australia. *Catena* 134, 4–13.
- Yaalon, D.H., 1981. Environmental Setting. In: Dan, J., Gerson, R., Koyumdjisky, H., Yaalon, D.H. (Eds.), *Aridic Soils of Israel: Properties, Genesis and Management*. Agricultural Research Organization, Institute of Soils and Water, Bet Dagan, Israel, pp. 3–16.
- Yaalon, D.H., 2000. Soil Care Attitudes and Strategies of Land Use through Human History. *SARTONIANA*, George Sarton Chair of the History of Sciences 13. University of Ghent, Ghent, pp. 147–159 (1999–2000).
- Yaalon, D.H., Dan, J., 1974. Accumulation and distribution of loess-derived deposits in the semi-desert and desert fringe areas of Israel. *Z. f. Geomorphol. N.F.* 20, 91–105.
- Yaalon, D.H., Ganor, E., 1973. The influence of dust on the soils during the quaternary. *Soil Sci.* 116, 146–155.
- Yair, A., Enzel, Y., 1987. The Relationship between Annual Rainfall and Sediment Yield in Arid and Semi-Arid Areas. The Case of the Northern Negev. *Catena (Suppl. 10)*, 121–135.
- Zilberman, E., 1992. The late Pleistocene sequence of the northwestern Negev flood plains – a key to reconstructing the paleoclimate of southern Israel in the last glacial. *Isr. J. Earth Sci.* 41, 155–167.